11

Numerical Analysis of the ElectromagneticShielding Effect of Reinforced Concrete Walls

Gaobiao Xiao and Junfa Mao
Shanghai Jiao Tong University
P.R. China

1. Introduction

The shielding effect of buildings to electromagnetic waves is investigated by many researchers (Dalke etal., 2000), where the analysis of reinforced concrete walls has attracted special interests. In most cases, a reinforced concrete wall is treated as an infinitely extended periodic structure and periodic boundary conditions are used to get its transmission and reflection characteristics, from which the shielding effect of the wall can be evaluated. However, when analyzing indoor electro-magnetic environment, the surrounding reinforced concrete walls are not infinitely extended. Therefore, the infinitely extending plane structure model cannot provide an accurate enough prediction to the indoor electromagnetic environment, especially the fields at corners or ends of walls. Some numerical methods, such as method of moment (MoM) seem to be applicable for analyzing these kinds of problems. However, the computational cost may be too high since these kinds of electromagnetic systems usually not only have electrical sizes of tens or hundreds wavelengths, but also have very fine internal structures.

In this chapter, we present a method to circumvent the heavy burden on computing sources while adequate accuracy can still be achieved. A reinforced concrete wall with fine structures is first divided into small blocks. Each block is treated like a multi-layered scatterer and is analyzed independently by using cascaded network techniques. Then, the electromagnetic characteristics of that block is expressed by a generalized transition matrix (generalized T-matrix, GTM) that is defined on a specified reference surface containing the block, which is different from the T-matrix introduced by Waterman (Waterman, 2007). The mutual coupling effects among blocks are evaluated by using the generalized transition matrices of all blocks directly. The scattered fields of the whole system are calculated using a generalized surface integral equation method (GSIE). Furthermore, we will show that characteristic basis functions (CBF) and synthetic basis functions (SBF) can be used to accelerate the evaluation process effectively.

The following contents are included in this chapter: (1) description of the basic concept of generalized transition matrix and the generalized surface integral equation method, (2) the cascading network technique in analyzing multi-layered media, (3) the implementation of

GSIE in conjunction with CBF\SBF, and (4) as an application example, the evaluation of the shielding effect of a 2D reinforced wall with the proposed method.

2. Generalized Surface Integral Equation

The electromagnetic problem under consideration is shown in Fig. 1. A 2-D cavity is surrounded by a $10\lambda \times 10\lambda$ concrete wall. The wall is 1.0λ thick and is uniformly reinforced by 36 circular steel cylinders with radius of 0.1λ and conductivity of $\sigma = 1.1\times 10^6$ Sm-1. The relative permittivity of the concrete is $\varepsilon_r = 10 - j2.8$. The excitation is assumed to be a TM type plane wave with incident angle of ϕ.

In order to calculate the electromagnetic fields in the cavity, the wall is divided into 36 cells. Each cell consists of a steel cylinder and a concentric concrete cylinder with square cross section of $1.0\lambda \times 1.0\lambda$, as is sketched in Fig. 1. A cell is a multilayered scatterer and its scattering characteristics can be fully described by a generalized transition matrix, which relates the scattered tangential fields to the incident tangential fields directly, as is shown in Fig. 2.

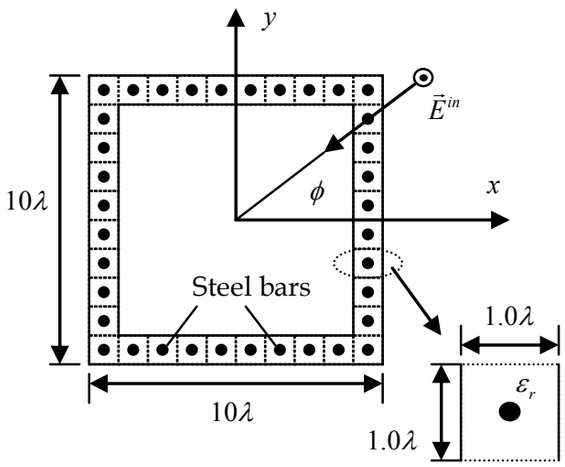

Fig. 1. A 2-D cavity surrounded by a concrete wall. The wall is uniformly reinforced by 36 circular steel cylinders with radius of 0.1λ and conductivity of $1.1\times 10^6 \mathrm{Sm}^{-1}$.

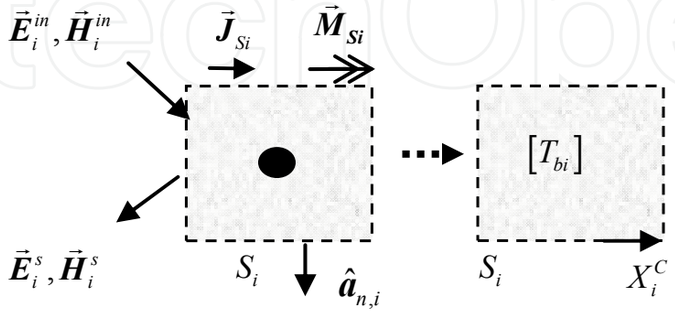

Fig. 2. A block is modelled with its associated generalized transition matrix $[T_{bi}]$. $\vec{J}_{Si}$ and $\vec{M}_{Si}$ are equivalent surface electric current and magnetic current, respectively.

A scatterer with two layers of homogeneous media is illustrated in Fig. 3(a), where V_1 denotes the medium between interface S_1 and S_2, with permittivity ε_1 and permeability μ_1. For a block of the concrete wall, S_1 is the air-concrete interface and S_2 the concrete-steel interface. The normal unit vectors of all interfaces are chosen to point outwardly. The outermost medium, denoted by V_0 is assumed to be free space.

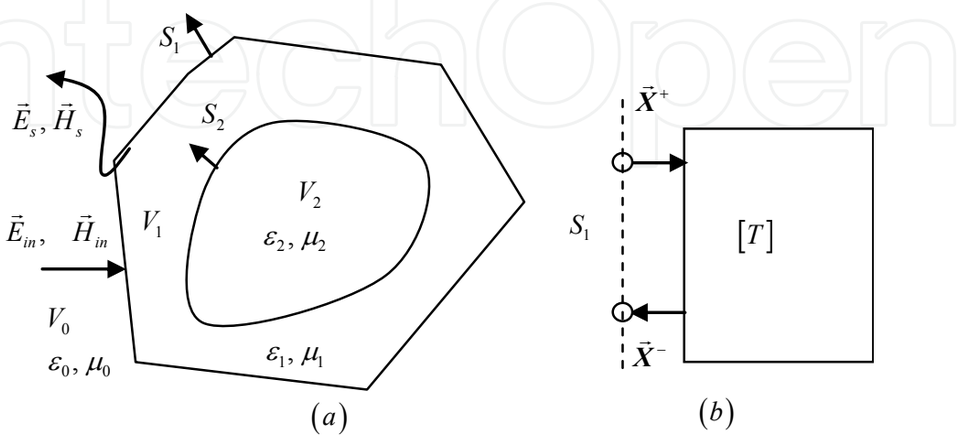

Fig. 3. (a) A scatterer with two layers. (b) One-port device model.

We examine the field scattering problem on interface S_1 at first. The incident fields may come from both sides of the interface, and being scattered to both sides of it, as is shown in Fig. 4(a). The interface may be modelled as a generalized two-port device, with its two reference surfaces being chosen as S_1^+ and S_1^-. The notation S_1^+ means approaching S_1 from outside while S_1^- means approaching S_1 from interior area.

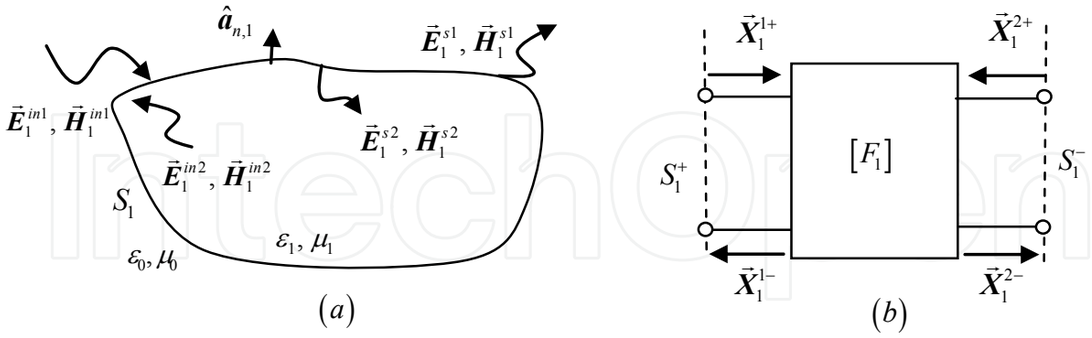

Fig. 4. (a) Scattering on interface S_1, with incident fields from both sides of it. (b) Generalized two-port device model, with its two reference surfaces approaching S_1 from outer or interior medium.

Define the rotated tangential components of incident fields and rotated tangential components of scattered fields of a block as follows (Xiao et al., 2008):

$$\left[\vec{X}_1^{1+}\right]=\begin{bmatrix}\vec{E}_1^{1+}\\ \vec{H}_1^{1+}\end{bmatrix}=\begin{bmatrix}-\hat{a}_{n,1}\times\vec{E}_1^{in1}\\ \hat{a}_{n,1}\times\vec{H}_1^{in1}\end{bmatrix}\Bigg|_{S_1^+}, \tag{1}$$

$$\left[\vec{X}_1^{2+}\right]=\begin{bmatrix}\vec{E}_1^{2+}\\ \vec{H}_1^{2+}\end{bmatrix}=\begin{bmatrix}\hat{a}_{n,1}\times\vec{E}_1^{in2}\\ -\hat{a}_{n,1}\times\vec{H}_1^{in2}\end{bmatrix}\Bigg|_{S_1^-}, \tag{2}$$

$$\left[\vec{X}_1^{1-}\right]=\begin{bmatrix}\vec{E}_1^{1-}\\ \vec{H}_1^{1-}\end{bmatrix}=\begin{bmatrix}-\hat{a}_{n,1}\times\vec{E}_1^{s1}\\ \hat{a}_{n,1}\times\vec{H}_1^{s1}\end{bmatrix}\Bigg|_{S_1^+}, \tag{3}$$

$$\left[\vec{X}_1^{2-}\right]=\begin{bmatrix}\vec{E}_1^{2-}\\ \vec{H}_1^{2-}\end{bmatrix}=\begin{bmatrix}\hat{a}_{n,1}\times\vec{E}_1^{s2}\\ -\hat{a}_{n,1}\times\vec{H}_1^{s2}\end{bmatrix}\Bigg|_{S_1^-}. \tag{4}$$

Note that the normal unit vector for S_1^- is chosen to be $-\hat{a}_{n,1}$. Based on Huygens' equivalence source principle, the scattered fields from interface S_1 can be expressed in terms of their tangential fields on the interface using the dyadic Green's function,

$$\vec{E}_1^{s1}(\vec{r})=\int_{S_1}\left[-j\omega\mu_0\overline{\overline{G}}_0\bullet\vec{H}_1^{1-}-\nabla\times\overline{\overline{G}}_0\bullet\vec{E}_1^{1-}\right]dS', \tag{5}$$

$$\vec{H}_1^{s1}(\vec{r})=\int_{S_1}\left[-j\omega\varepsilon_0\overline{\overline{G}}_0\bullet\vec{E}_1^{1-}+\nabla\times\overline{\overline{G}}_0\bullet\vec{H}_1^{1-}\right]dS', \tag{6}$$

$$\vec{E}_1^{s2}(\vec{r})=\int_{S_1}\left[-j\omega\mu_1\overline{\overline{G}}_1\bullet\vec{H}_1^{2-}-\nabla\times\overline{\overline{G}}_1\bullet\vec{E}_1^{2-}\right]dS', \tag{7}$$

$$\vec{H}_1^{s2}(\vec{r})=\int_{S_1}\left[-j\omega\varepsilon_1\overline{\overline{G}}_1\bullet\vec{E}_1^{2-}+\nabla\times\overline{\overline{G}}_1\bullet\vec{H}_1^{2-}\right]dS', \tag{8}$$

where $\overline{\overline{G}}_l=\left(\overline{\overline{I}}+\frac{\nabla\nabla}{k_l^2}\right)g_l$ is the dyadic Green's function, and g_l is the scalar Green's function in medium V_l, $k_l=\omega\sqrt{\mu_l\varepsilon_l}$ and $l=0,1$. The fields have to satisfy the following boundary conditions on interface S_1,

$$\vec{E}_1^{1+}+\vec{E}_1^{1-}=-\vec{E}_1^{2+}-\vec{E}_1^{2-}\quad,\qquad \vec{H}_1^{1+}+\vec{H}_1^{1-}=-\vec{H}_1^{2+}-\vec{H}_1^{2-}\quad. \tag{9}$$

Take the scattered electric field expressed by (5) as an example. If we move the observation point to surface S_1 from the outside area, and take into account the singularities of the dyadic Green's functions when source and observation points overlap, the rotated tangential scattered electric field on surface S_1^+ can be written as

$$\vec{\boldsymbol{E}}_1^{1-} = -\hat{\boldsymbol{a}}_{n,1} \times \vec{\boldsymbol{E}}_1^{s1}\Big|_{S_1^+} = -\hat{\boldsymbol{a}}_{n,1} \times \int_{S_1} \left(-j\omega\mu_0 \overline{\overline{\boldsymbol{G}}}_0\right) \bullet \vec{\boldsymbol{H}}_1^{1-} dS' - \hat{\boldsymbol{a}}_{n,1} \times \int_{S_1} \left(-\nabla g_0 \times \vec{\boldsymbol{E}}_1^{1-}\right) dS' + \frac{\Omega}{4\pi} \vec{\boldsymbol{E}}_1^{1-} \quad . \quad (10)$$

For smooth surface, the solid angle is $\Omega = 2\pi$, equation (10) becomes

$$\frac{1}{2} \vec{\boldsymbol{E}}_1^{1-} = \hat{\boldsymbol{a}}_{n,1} \times \int_{S_1} \nabla g_0 \times \vec{\boldsymbol{E}}_1^{1-} dS' + \hat{\boldsymbol{a}}_{n,1} \times \int_{S_1} \left(j\omega\mu_0 \overline{\overline{\boldsymbol{G}}}_0\right) \bullet \vec{\boldsymbol{H}}_1^{1-} dS' . \quad (11)$$

If we examine the scattered electric field $\vec{\boldsymbol{E}}_1^{s2}(\vec{r})$ and move the observation point to surface S_1 from its interior area, we can show that the rotated tangential scattered electric field on S_1^- satisfies

$$-\frac{1}{2} \vec{\boldsymbol{E}}_1^{2-} = \hat{\boldsymbol{a}}_{n,1} \times \int_{S_1} \nabla g_1 \times \vec{\boldsymbol{E}}_1^{2-} dS' + \hat{\boldsymbol{a}}_{n,1} \times \int_{S_1} \left(j\omega\mu_1 \overline{\overline{\boldsymbol{G}}}_1\right) \bullet \vec{\boldsymbol{H}}_1^{2-} dS' . \quad (12)$$

Integral equations for rotated tangential magnetic fields can be expressed in similar way,

$$\frac{1}{2} \vec{\boldsymbol{H}}_1^{1-} = -\hat{\boldsymbol{a}}_{n,1} \times \int_{S_1} \left(j\omega\varepsilon_0 \overline{\overline{\boldsymbol{G}}}_0\right) \bullet \vec{\boldsymbol{E}}_1^{1-} dS' + \hat{\boldsymbol{a}}_{n,1} \times \int_{S_1} \nabla g_0 \times \vec{\boldsymbol{H}}_1^{1-} dS' \quad , \quad (13)$$

$$-\frac{1}{2} \vec{\boldsymbol{H}}_1^{2-} = -\hat{\boldsymbol{a}}_{n,1} \times \int_{S_1} \left(j\omega\varepsilon_1 \overline{\overline{\boldsymbol{G}}}_1\right) \bullet \vec{\boldsymbol{E}}_1^{2-} dS' + \hat{\boldsymbol{a}}_{n,1} \times \int_{S_1} \nabla g_1 \times \vec{\boldsymbol{H}}_1^{2-} dS' \quad . \quad (14)$$

The same process can also be applied to the incident fields. For example, according to the Huygens' principle and the distinction theorem, we have

$$-\frac{1}{2} \vec{\boldsymbol{E}}_1^{1+} = \hat{\boldsymbol{a}}_{n,1} \times \int_{S_1} \nabla g_0 \times \vec{\boldsymbol{E}}_1^{1+} dS' + \hat{\boldsymbol{a}}_{n,1} \times \int_{S_1} \left(j\omega\mu_0 \overline{\overline{\boldsymbol{G}}}_0\right) \bullet \vec{\boldsymbol{H}}_1^{1+} dS' \quad , \quad (15)$$

$$-\frac{1}{2} \vec{\boldsymbol{H}}_1^{1+} = -\hat{\boldsymbol{a}}_{n,1} \times \int_{S_1} \left(j\omega\varepsilon_0 \overline{\overline{\boldsymbol{G}}}_0\right) \bullet \vec{\boldsymbol{E}}_1^{1+} dS' + \hat{\boldsymbol{a}}_{n,1} \times \int_{S_1} \nabla g_0 \times \vec{\boldsymbol{H}}_1^{1+} dS' \quad . \quad (16)$$

With these integral equations, we are able to establish a set of coupled surface integral equations on interface S_1 . Firstly, we consider the case that an incident field illuminates on S_1 from the outer side only, *i.e.*, $\vec{\boldsymbol{X}}_1^{1+} \neq 0,\ \vec{\boldsymbol{X}}_1^{2+} = 0$. Combining (11)-(16) and eliminating $\vec{\boldsymbol{E}}_1^{1-}, \vec{\boldsymbol{H}}_1^{1-}$ gives

$$\hat{\boldsymbol{a}}_{n,1} \times \int_{S_1} \nabla\left(g_0 + g_1\right) \times \vec{\boldsymbol{E}}_1^{2-} dS' + \hat{\boldsymbol{a}}_{n,1} \times \int_{S_1} \left(j\omega\mu_0 \overline{\overline{\boldsymbol{G}}}_0 + j\omega\mu_1 \overline{\overline{\boldsymbol{G}}}_1\right) \bullet \vec{\boldsymbol{H}}_1^{2-} dS' = \vec{\boldsymbol{E}}_1^{1+} \quad , \quad (17)$$

$$-\hat{\boldsymbol{a}}_{n,1} \times \int_{S_1} \left(j\omega\varepsilon_0 \overline{\overline{\boldsymbol{G}}}_0 + j\omega\varepsilon_1 \overline{\overline{\boldsymbol{G}}}_1\right) \bullet \vec{\boldsymbol{E}}_1^{2-} dS' + \hat{\boldsymbol{a}}_{n,1} \times \int_{S_1} \nabla\left(g_0 + g_1\right) \times \vec{\boldsymbol{H}}_1^{2-} dS' = \vec{\boldsymbol{H}}_1^{1+} \quad . \quad (18)$$

It is not difficult to check that (17) and (18) are equivalent to PMCHW formulation (Rao etal., 1982) by denoting $\vec{J}_s = \vec{H}^{2-}$, $\vec{J}_{ms} = \vec{E}^{2-}$. Symbolically, the rotated tangential scattered fields on interface S_1^- can be expressed in terms of the incident fields as

$$\left[\vec{X}_1^{2-}\right] = \left[\tau_1(\cdot)\right]\left[\vec{X}_1^{1+}\right]. \tag{19}$$

Therefore, the rotated tangential scattered fields on interface S_1^+ is obtained by

$$\left[\vec{X}_1^{1-}\right] = -\left\{\boldsymbol{I} + \left[\tau_1(\cdot)\right]\right\}\left[\vec{X}_1^{1+}\right]. \tag{20}$$

$\boldsymbol{I}$ is the identity tensor. It is natural to interpret $\left[\tau_1(\cdot)\right]$ as a transmission operator and $\left[\mathcal{T}(\cdot)\right] = -\left\{\boldsymbol{I} + \left[\tau_1(\cdot)\right]\right\}$ a reflection operator.

Secondly, we consider the case that incident field illuminates on S_1 from interior side only, i.e., $\vec{X}^{1+} = 0,\ \vec{X}^{2+} \neq 0$. It can be proven that the rotated tangential scattered fields are subject to the following coupled surface integral equations,

$$\hat{\boldsymbol{a}}_{n,1} \times \int_{S_1} \nabla\left(g_0 + g_1\right) \times \vec{\boldsymbol{E}}_1^{1-} dS' + \hat{\boldsymbol{a}}_{n,1} \times \int_{S_1} \left(-j\omega\mu_0 \overline{\overline{\boldsymbol{G}}}_0 - j\omega\mu_1 \overline{\overline{\boldsymbol{G}}}_1\right) \bullet \vec{\boldsymbol{H}}_1^{1-} dS' = -\vec{\boldsymbol{E}}_1^{2+} \quad , \tag{21}$$

$$\hat{\boldsymbol{a}}_{n,1} \times \int_{S_1} \left(j\omega\varepsilon_0 \overline{\overline{\boldsymbol{G}}}_0 + j\omega\varepsilon_1 \overline{\overline{\boldsymbol{G}}}_1\right) \bullet \vec{\boldsymbol{E}}_1^{1-} dS' + \hat{\boldsymbol{a}}_{n,1} \times \int_{S_1} \nabla\left(g_0 + g_1\right) \times \vec{\boldsymbol{H}}_1^{1-} dS' = -\vec{\boldsymbol{H}}_1^{2+}. \tag{22}$$

Comparing (21) (22) with (17) (18), we can write that

$$\left[\vec{X}_1^{1-}\right] = -\left[\tau_1(\cdot)\right]\left[\vec{X}_1^{2+}\right], \tag{23}$$

$$\left[\vec{X}_1^{2-}\right] = \left\{-\boldsymbol{I} + \left[\tau_1(\cdot)\right]\right\}\left[\vec{X}_1^{2+}\right]. \tag{24}$$

In general situations, incident fields come from both sides of an interface, the total scattered fields are obtained by field superposition, which can be written in matrix form as

$$\begin{bmatrix} \vec{X}_1^{1-} \\ \vec{X}_1^{2-} \end{bmatrix} = \begin{bmatrix} -\left\{\boldsymbol{I} + \left[\tau_1(\cdot)\right]\right\} & -\left[\tau_1(\cdot)\right] \\ \left[\tau_1(\cdot)\right] & -\boldsymbol{I} + \left[\tau_1(\cdot)\right] \end{bmatrix} \begin{bmatrix} \vec{X}_1^{1+} \\ \vec{X}_1^{2+} \end{bmatrix}. \tag{25}$$

It can be re-arranged in field transfer equation,

$$\begin{bmatrix} \vec{X}_1^{1+} \\ \vec{X}_1^{1-} \end{bmatrix} = \left[\mathcal{F}_1(\cdot)\right] \begin{bmatrix} \vec{X}_1^{2+} \\ \vec{X}_1^{2-} \end{bmatrix}, \tag{26}$$

where $\left[\mathcal{F}_l(\cdot)\right]$ may be interpreted as a transfer operator.

The scattered fields $\vec{\boldsymbol{E}}_1^{s2}, \vec{\boldsymbol{H}}_1^{s2}$ will transfer to interface S_2 and serve as the incident fields on S_2, i.e., $\vec{\boldsymbol{E}}_2^{1+}, \vec{\boldsymbol{H}}_2^{1+}$, as is illustrated in Fig. 5. Similarly, the scattered fields $\vec{\boldsymbol{E}}_2^{1-}, \vec{\boldsymbol{H}}_2^{1-}$ from interface S_2 will transmit through the medium layer and illuminate on S_1 as the incident fields of $\vec{\boldsymbol{E}}_1^{2+}, \vec{\boldsymbol{H}}_1^{2+}$. From Huygens' principle, the scattered fields associated with $\vec{\boldsymbol{E}}_1^{2-}, \vec{\boldsymbol{H}}_1^{2-}$ are

$$\vec{\boldsymbol{E}}_1^{s2}(\vec{\boldsymbol{r}}) = -\int_{S_1}\left(\nabla g_1 \times \vec{\boldsymbol{E}}_1^{2-}\right)dS' + \int_{S_1}\left(-j\omega\mu_1\overline{\overline{\boldsymbol{G}}}_1\right)\bullet\vec{\boldsymbol{H}}_1^{2-}dS', \tag{27}$$

$$\vec{\boldsymbol{H}}_1^{s2}(\vec{\boldsymbol{r}}) = -\int_{S_1}\left(j\omega\varepsilon_1\overline{\overline{\boldsymbol{G}}}_1\right)\bullet\vec{\boldsymbol{E}}_1^{2-}dS' + \int_{S_1}\nabla g_1 \times \vec{\boldsymbol{H}}_1^{2-}dS'. \tag{28}$$

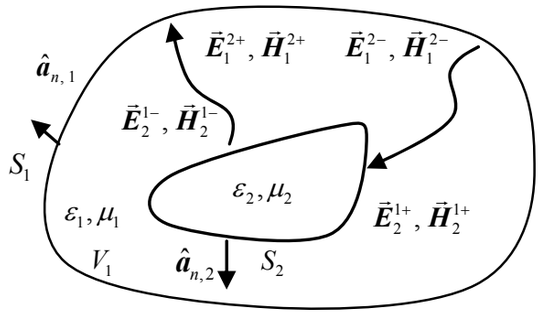

Fig. 5. Field transmission between interface S_1 and S_2.

Using the definition of rotated tangential components, we get

$$\vec{\boldsymbol{E}}_2^{1+} = -\hat{\boldsymbol{a}}_{n,2}\times\vec{\boldsymbol{E}}_1^{s2}\left(\vec{\boldsymbol{r}}_2^{+}\right) = \hat{\boldsymbol{a}}_{n,2}\times\int_{S_1}\left(\nabla g_1\times\vec{\boldsymbol{E}}_1^{2-}\right)dS' + \hat{\boldsymbol{a}}_{n,2}\times\int_{S_1}\left(j\omega\mu_1\overline{\overline{\boldsymbol{G}}}_1\right)\bullet\vec{\boldsymbol{H}}_1^{2-}dS', \tag{29}$$

$$\vec{\boldsymbol{H}}_2^{1+} = \hat{\boldsymbol{a}}_{n,2}\times\vec{\boldsymbol{H}}_1^{s2}\left(\vec{\boldsymbol{r}}_2^{+}\right) = -\hat{\boldsymbol{a}}_{n,2}\times\int_{S_1}\left(j\omega\varepsilon_1\overline{\overline{\boldsymbol{G}}}_1\right)\bullet\vec{\boldsymbol{E}}_1^{2-}dS' + \hat{\boldsymbol{a}}_{n,2}\times\int_{S_1}\nabla g_1\times\vec{\boldsymbol{H}}_1^{2-}dS'. \tag{30}$$

Equations (29) and (30) describe the field transmission from $\vec{\boldsymbol{E}}_1^{2-}, \vec{\boldsymbol{H}}_1^{2-}$ to $\vec{\boldsymbol{E}}_2^{1+}, \vec{\boldsymbol{H}}_2^{1+}$. Similarly, the relationship between the incident fields on the inner side of S_1 and the scattered fields from S_2 can be derived as

$$\vec{\boldsymbol{E}}_1^{2+} = -\hat{\boldsymbol{a}}_{n,1}\times\int_{S_2}\nabla g_1\times\vec{\boldsymbol{E}}_2^{1-}dS' - \hat{\boldsymbol{a}}_{n,1}\times\int_{S_2}\left(j\omega\mu_1\overline{\overline{\boldsymbol{G}}}_1\right)\bullet\vec{\boldsymbol{H}}_2^{1-}dS', \tag{31}$$

$$\vec{\boldsymbol{H}}_1^{2+} = \hat{\boldsymbol{a}}_{n,1}\times\int_{S_2}\left(j\omega\varepsilon_1\overline{\overline{\boldsymbol{G}}}_1\right)\bullet\vec{\boldsymbol{E}}_2^{1-}dS' - \hat{\boldsymbol{a}}_{n,1}\times\int_{S_2}\nabla g_1\times\vec{\boldsymbol{H}}_2^{1-}dS'. \tag{32}$$

Symbolically we denote

$$\left[\vec{\boldsymbol{X}}_1^{2+}\right] = \left[\mathcal{D}_{12}(\cdot)\right]\left[\vec{\boldsymbol{X}}_2^{1-}\right], \tag{33}$$

$$\left[\vec{\boldsymbol{X}}_2^{1+}\right]=\left[\mathcal{D}_{21}(\cdot)\right]\left[\vec{\boldsymbol{X}}_1^{2-}\right]. \tag{34}$$

(33) and (34) depict the relationship between the fields of two consecutive interfaces, with $\left[\mathcal{D}_{ij}(\cdot)\right]$ being the transmission operator. The first subscript of $\left[\mathcal{D}(\cdot)\right]$ indicates the destination interface, while the second subscript indicates the source interface. This convention is used throughout this chapter. Obviously, the homogeneous medium layer can be considered as a section of generalized transmission line, with $\left[\mathcal{D}_{21}(\cdot)\right]$ and $\left[\mathcal{D}_{12}(\cdot)\right]$ being its forward and backward transmission operators, respectively.

Since the innermost layer V_2 is homogeneous, the scattering problem on S_2 can be considered as a special case of the above scattering problem with $\vec{\boldsymbol{X}}_2^{2+}=0$. The scattered fields are only related to the incident fields from the outer side of the interface by equation (20), which is rewritten as follows

$$\left[\vec{\boldsymbol{X}}_2^{1-}\right]=-\left\{\boldsymbol{I}+\left[\tau_2(\cdot)\right]\right\}\left[\vec{\boldsymbol{X}}_2^{1+}\right]=\left[\mathcal{T}_2(\cdot)\right]\left[\vec{\boldsymbol{X}}_2^{1+}\right]. \tag{35}$$

Therefore, the two-layered scatterer is modelled as a cascaded network of two generalized devices connected by a transmission line, as is shown in Fig. 6.

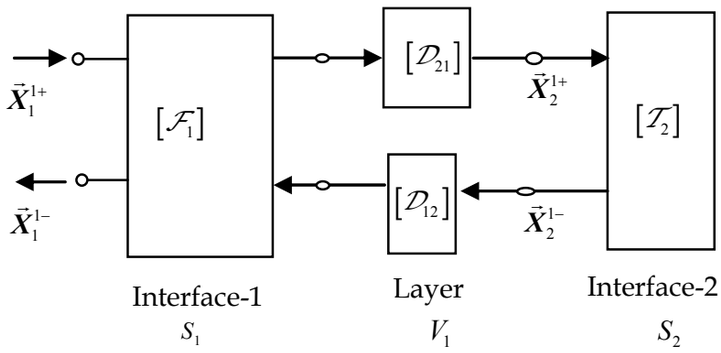

Fig. 6 A cascaded network model for a two-layered scatterer.

Assume that all field components are expanded and tested with a kind of vector basis functions on the reference surface *S*. The generalized transition matrix $[T_{bi}]$ of block *i* is defined according to

$$\left[X_i^-\right]=\left[T_{bi}\right]\left[X_i^+\right]. \tag{36}$$

$[T_b]$ can be used to describe the scattering characteristics of a scatterer with arbitrary shapes and materials. At a given frequency, $[T_b]$ is calculated independently only once for each block and can be re-used if necessary. For homogeneous media, the entries of $[T_b]$ can be found from (17), (18) by applying Galerkin's scheme directly. For scatterers with complex

structures, $[T_b]$ may be obtained using properly chosen method (Creticos & Schaubert, 2006; Lean, 2004; Polewski etal., 2004; Taskinen & Ylä-Oijala, 2006; Umashankar etal.,1986;). In this chapter, the generalized transition matrix of a two-layered block is obtained using the above described cascaded network technique.

Assume that all rotated tangential fields on the interface S_l are expanded with a set of vector basis functions $\vec{\boldsymbol{f}}_{l,j}(\boldsymbol{r})$ as follows:

$$\vec{\boldsymbol{E}}_l^{u\pm}(\boldsymbol{r}) = \sum_{i=1}^{N_l} e_{l,j}^{u\pm}\vec{\boldsymbol{f}}_{l,j}(\boldsymbol{r}), \qquad \vec{\boldsymbol{H}}_l^{u\pm}(\boldsymbol{r}) = \sum_{j=1}^{N_l} h_{l,j}^{u\pm}\vec{\boldsymbol{f}}_{l,j}(\boldsymbol{r}), \tag{37}$$

where N_l is number of vector functions used on interface S_l and $u = 1,2$. Functions $\vec{\boldsymbol{f}}_{l,i}(\boldsymbol{r})$ are also used as test functions. For the sake of convenience, we denote

$$\tilde{e}_{l,i}^{u\pm} = \int_{t_i} \vec{\boldsymbol{E}}_l^{u\pm}(\boldsymbol{r})\bullet\vec{\boldsymbol{f}}_{l,i}(\boldsymbol{r})\,dS, \qquad \tilde{h}_{l,i}^{u\pm} = \int_{t_i} \vec{\boldsymbol{H}}_l^{u\pm}(\boldsymbol{r})\bullet\vec{\boldsymbol{f}}_{l,i}(\boldsymbol{r})\,dS, \tag{38}$$

where t_i is the support of vector basis function $\vec{\boldsymbol{f}}_{l,i}(\boldsymbol{r})$. It can be derived that

$$\left[\tilde{e}_l^{u\pm}\right] = [\boldsymbol{P}_l]\left[e_l^{u\pm}\right], \quad \left[\tilde{h}_l^{u\pm}\right] = [\boldsymbol{P}_l]\left[h_l^{u\pm}\right]. \tag{39}$$

Here $[\boldsymbol{P}_l]$ is a Gramm matrix formed by the inner products of the basis functions and test functions on the surface S_l. The entries of the Gramm matrix are defined as

$$P_l(i,j) = \int_{t_i} \vec{\boldsymbol{f}}_{l,j}(\boldsymbol{r})\bullet\vec{\boldsymbol{f}}_{l,i}(\boldsymbol{r})dS. \tag{40}$$

Applying Galerkin's method to (17) (18) yields

$$\begin{bmatrix}\left[\boldsymbol{A}_l^{ee}\right] & \left[\boldsymbol{A}_l^{eh}\right]\\ \left[\boldsymbol{A}_l^{he}\right] & \left[\boldsymbol{A}_l^{hh}\right]\end{bmatrix}\begin{bmatrix}\left[e_l^{2-}\right]\\ \left[h_l^{2-}\right]\end{bmatrix} = \begin{bmatrix}\left[\tilde{e}_l^{1+}\right]\\ \left[\tilde{h}_l^{1+}\right]\end{bmatrix} = \begin{bmatrix}[\boldsymbol{P}_l] & 0\\ 0 & [\boldsymbol{P}_l]\end{bmatrix}\begin{bmatrix}\left[e_l^{1+}\right]\\ \left[h_l^{1+}\right]\end{bmatrix}, \tag{41}$$

where all elements of the coefficient matrices have their conventional form of double surface integrations on the corresponding meshes. For example, on S_1 we have

$$\boldsymbol{A}_1^{ee}(i,j) = \int_{t_i} \vec{\boldsymbol{f}}_{1,i}(\boldsymbol{r})\bullet\hat{\boldsymbol{a}}_{n,1}\times\int_{t_j}\nabla(g_0+g_1)\times\vec{\boldsymbol{f}}_{1,j}(\boldsymbol{r})\,dS'dS. \tag{42}$$

A generalized transmission matrix $[\boldsymbol{\tau}_l]$ can be defined as

$$[\boldsymbol{\tau}_l]=\begin{bmatrix}[\boldsymbol{A}_l^{ee}] & [\boldsymbol{A}_l^{eh}]\\ [\boldsymbol{A}_l^{he}] & [\boldsymbol{A}_l^{hh}]\end{bmatrix}^{-1}\begin{bmatrix}[\boldsymbol{P}_l] & 0\\ 0 & [\boldsymbol{P}_l]\end{bmatrix}\triangleq[\boldsymbol{A}_l]^{-1}[\boldsymbol{P}_{cl}]. \tag{43}$$

Although $[\boldsymbol{\tau}_l]$ is frequency-dependent, it does not depend on incident fields. The generalized transfer matrix of interface S_l can then be defined accordingly,

$$[\boldsymbol{F}_l]=\begin{bmatrix}[\boldsymbol{F}_l^{11}] & [\boldsymbol{F}_l^{12}]\\ [\boldsymbol{F}_l^{21}] & [\boldsymbol{F}_l^{22}]\end{bmatrix}=\begin{bmatrix}[\boldsymbol{\tau}_l]^{-1}-\boldsymbol{I} & [\boldsymbol{\tau}_l]^{-1}\\ -[\boldsymbol{\tau}_l]^{-1} & -[\boldsymbol{\tau}_l]^{-1}-\boldsymbol{I}\end{bmatrix}=\begin{bmatrix}[\boldsymbol{P}_{cl}]^{-1}[\boldsymbol{A}_l]-\boldsymbol{I} & [\boldsymbol{P}_{cl}]^{-1}[\boldsymbol{A}_l]\\ -[\boldsymbol{P}_{cl}]^{-1}[\boldsymbol{A}_l] & -[\boldsymbol{P}_{cl}]^{-1}[\boldsymbol{A}_l]-\boldsymbol{I}\end{bmatrix}. \tag{44}$$

The same mesh structure and vector basis functions are applied when evaluate field transmission between consecutive interfaces. We still consider the two-layered scatterer shown in Fig. 5. Applying Galerkin's method to integral equations (29)-(32) yields

$$[\boldsymbol{P}_{c1}]\left[\vec{\boldsymbol{X}}_1^{2+}\right]=[\boldsymbol{D}_{12}]\left[\vec{\boldsymbol{X}}_2^{1-}\right], \tag{45}$$

$$[\boldsymbol{P}_{c2}]\left[\vec{\boldsymbol{X}}_2^{1+}\right]=[\boldsymbol{D}_{21}]\left[\vec{\boldsymbol{X}}_1^{2-}\right], \tag{46}$$

where $[\boldsymbol{D}_{21}]$ is the field transmission matrix from interface S_2 to S_1.
Tracing the field transmission route illustrated in Fig. 5 leads to,

$$[\boldsymbol{P}_{c1}]\left[\vec{\boldsymbol{X}}_1^{2+}\right]=[\boldsymbol{P}_{c1}][\boldsymbol{D}_{12}]\left[\vec{\boldsymbol{X}}_2^{1-}\right]=[\boldsymbol{P}_{c1}][\boldsymbol{D}_{12}][\Gamma_2]\left[\vec{\boldsymbol{X}}_2^{1-}\right]=[\boldsymbol{P}_{c1}][\boldsymbol{D}_{12}][T_2][\boldsymbol{P}_{c2}]^{-1}[\boldsymbol{D}_{21}]\left[\vec{\boldsymbol{X}}_1^{2-}\right]. \tag{47}$$

Denote

$$\left[\Gamma_1^-\right]=[\boldsymbol{D}_{12}][T_2][\boldsymbol{P}_{c2}]^{-1}[\boldsymbol{D}_{21}]\left[\vec{\boldsymbol{X}}_1^{2-}\right]. \tag{48}$$

The generalized T-matrix for a bock is found to be

$$[T_b]=\left(\left[\boldsymbol{F}_1^{21}\right]\left[\Gamma_1^-\right]+\left[\boldsymbol{F}_1^{22}\right]\right)\left(\left[\boldsymbol{F}_1^{11}\right]\left[\Gamma_1^-\right]+\left[\boldsymbol{F}_1^{12}\right]\right)^{-1}. \tag{49}$$

Generally speaking, a multilayered scatterer can also be handled in this recursive way. A multilayered scatterer interacts with the surrounding environment all through the outermost interface. It is natural to use the generalized transition matrix $[\boldsymbol{T}]$ defined on the outermost interface to describe the whole scattering characteristics of the scatterer. For arbitrary incident fields, the rotated tangential scattered fields can be found from the rotated tangential incident fields directly by multiplying the generalized T-matrix.
This technique is used to analyse the block of the reinforced concrete wall. The scattering problem at the interface between concrete and air is solved by using surface integral equations (17)-(22), with its transfer matrix obtained by (44). The scattering problem at the surface of the steel bar is treated with the same approach. Coordinate transform may be

applied to overcome the numerical problem caused by high conductivity of the steel (Li & Chew, 2007). The generalized transition matrix $[T_2]$ of the steel bar is determined according to equation (20). The field transmission flow chart is illustrated in Fig. 7.

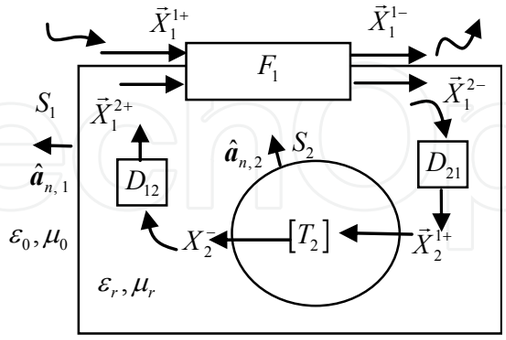

Fig. 7. Field transmission between interfaces S_1 and the surface of the steel core S_2.

After the scattering characteristics of all blocks are represented by their generalized T-matrices, the scattered fields of the whole wall can be analysed by taking into account of the mutual couplings between all blocks, as is shown in Fig. 8, where M scatterers are considered. The generalized transition matrix of scatterer m is denoted by $[T_m]$. It is defined on the reference surface S_m, and has been calculated independently in advance.

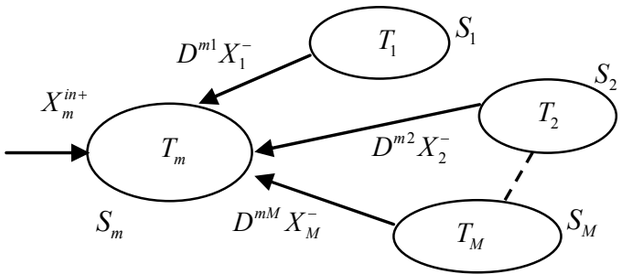

Fig.8 Total incident fields on scatterer-m, including the original incident fields and all scattered fields from other scatterers.

The total incident fields for scatterer-m include the original incident fields on its reference surface S_m and all scattered fields from other scatterers, *i.e.*,

$$\left[X_m^+\right] = \sum_{n=1,n\neq m}^{M} \left[P_{cm}\right]^{-1}\left[D_{mn}\right]\left[X_n^-\right] + \left[X_m^{in+}\right], \tag{50}$$

where $[D_{mn}]$ are field transmission matrix from scatterer-n to scatterer-m. They are defined like (29) (30), except that the integral areas are replaced by the corresponding reference surfaces of S_m and S_n. Denote

$$\left[D_{mn}\right] = \begin{bmatrix} \left[D_{mn}^{ee}\right] & \left[D_{mn}^{eh}\right] \\ \left[D_{mn}^{he}\right] & \left[D_{mn}^{hh}\right] \end{bmatrix}. \tag{51}$$

All entries are evaluated with double surface integrals. For example, we have

$$D_{mn}^{ee}(p,q)=\int_{t_p}\left[\hat{a}_{n,m}\times\int_{t_q}\nabla\times\overline{\overline{G}}_0\bullet\vec{f}_q(\boldsymbol{r}')dS_n\right]\bullet\vec{f}_p(\boldsymbol{r})dS_m\,, \tag{52}$$

where $\vec{f}_q(\boldsymbol{r}')$ and $\vec{f}_p(\boldsymbol{r})$ are basis functions on the reference surface of scatterer-n (source) and scatterer-m (destination), respectively, and $\hat{a}_{n,m}$ is the normal unit vector of S_m. $[P_{cm}]$ is the Gramm matrix on the surface of scatterer-m. The total scattered fields of scatterer-m on the specified reference surface is then obtained by $\left[X_m^-\right]=[T_m]\left[X_m^+\right]$. By virtue of equation (36) and the surface integral equations (17) (18), we can derive the discretized form of the surface integral equation defined on surface S_m as follows

$$\left[X_m^-\right]-\sum_{n=1,n\neq m}^{N_b}[T_n][D_{mn}]\left[X_n^-\right]=[T_m]\left[X_m^{inc}\right]. \tag{53}$$

$\left[\boldsymbol{X}_m^{inc}\right]$ is the original incident field on S_m. It can be proved that the equivalent sources satisfy a similar equation,

$$[I_{Sm}]-\sum_{n=1,m\neq n}^{N_b}[R_n][D_{mn}][I_{Sn}]=[R_n]\left[X_n^{inc}\right]. \tag{54}$$

Here N_b is the number of blocks, I_{Sm} are the expanding coefficient of equivalence surface sources, where $[R_n]=[I]+[T_n]$, $[I]$ is the identity tensor. Equation (53) or (54) is the matrix form of the generalized surface integral equation formulation of a complex multi-scale system. For perfect conducting surfaces, equation (54) is more convenient to use because $\vec{\boldsymbol{M}}_{Sm}=0$ in these cases. A complex multi-scale electromagnetic system may be divided into sub-blocks with proper sizes and reference surfaces. Small objects are usually grouped together and contained in one reference surface. Large bulk of inhomogeneous/homogeneous media or conducting media can be divided into smaller blocks. The generalized transition matrix of each block is then found using relevant method according to its structure; each block is assumed to be placed alone in the infinite homogeneous background media with parameters of ε_0 and μ_0. The total electromagnetic characteristics of the system can be evaluated using the generalized surface integral equations, i.e., equation (53) or (54). With this method, the unknowns involved in the final linear system are significantly reduced.

3. Field Transmission Matrices between Adjacent Blocks

Assume that block-m and block-n share a common interface S_{mn}, as is shown in Fig. 9, where $\hat{\boldsymbol{a}}_{n,m}$ and $\hat{\boldsymbol{a}}_{n,n}$ are normal unit vectors of surface S_m and S_n, respectively. The

scattered fields from block-m are expressed in terms of the rotated tangential fields on surface S_m using equations (5)-(6). Taking into account the singularity of the dyadic Green's function when the source point and observatory point overlap on surface S_{mn}, we can write that

$$\vec{\boldsymbol{E}}_{nm}^{+} = -\hat{\boldsymbol{a}}_{n,n} \times \vec{\boldsymbol{E}}_{m}^{s}(\vec{\boldsymbol{r}}) = \hat{\boldsymbol{a}}_{n,n} \times \int_{S_m} \left(j\omega\mu \overline{\overline{\boldsymbol{G}}}_0 \bullet \vec{\boldsymbol{H}}_m^{-} \right) \mathrm{d}S' + \hat{\boldsymbol{a}}_{n,n} \times \int_{S_m} \left(\nabla g_0 \times \vec{\boldsymbol{E}}_m^{-} \right) \mathrm{d}S' - \frac{\gamma}{2} \vec{\boldsymbol{E}}_m^{-}, \tag{55}$$

$$\vec{\boldsymbol{H}}_{nm}^{+} = \hat{\boldsymbol{a}}_{n,n} \times \vec{\boldsymbol{H}}^{s}(\vec{\boldsymbol{r}}) = -\hat{\boldsymbol{a}}_{n,n} \times \int_{S_m} j\omega\varepsilon \overline{\overline{\boldsymbol{G}}}_0 \bullet \vec{\boldsymbol{E}}_m^{-} \mathrm{d}S' + \hat{\boldsymbol{a}}_{n,n} \times \int_{S_m} \left(\nabla g_0 \times \vec{\boldsymbol{H}}_m^{-} \right) \mathrm{d}S' - \frac{\gamma}{2} \vec{\boldsymbol{H}}_m^{-}, \tag{56}$$

where $\vec{\boldsymbol{E}}_{nm}^{+}$ and $\vec{\boldsymbol{H}}_{nm}^{+}$ are the rotated tangential fields on S_n created by $\vec{\boldsymbol{E}}_m^{-}$ and $\vec{\boldsymbol{H}}_m^{-}$ on surface S_m. $\gamma = 1$ if $\vec{\boldsymbol{r}} \in S_{mn}$ and $\gamma = 0$ elsewhere. The fact that $\hat{\boldsymbol{a}}_{n,n} = -\hat{\boldsymbol{a}}_{n,m}$ on surface S_{mn} has been used to get equations (55) (56). Note that equations (55) and (56) also hold true if we replace $\vec{\boldsymbol{E}}_m^{-}$ by $\vec{\boldsymbol{M}}_{Sm}$ and $\vec{\boldsymbol{H}}_m^{-}$ by $\vec{\boldsymbol{J}}_{Sm}$ simultaneously.

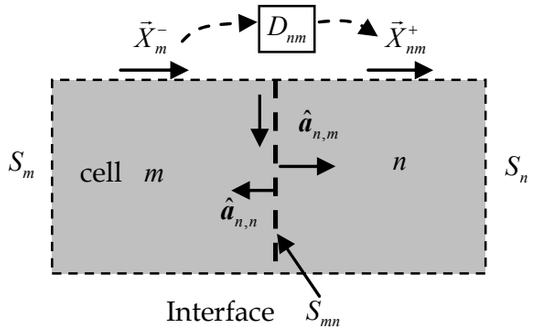

Fig. 9 Block-m and block-n share a common interface S_{mn}.

Assume that the rotated tangential fields are expanded and tested with vector basis functions $\vec{\boldsymbol{f}}_{m,j}$ and $\vec{\boldsymbol{f}}_{n,i}$ on surface S_m and S_n, respectively, then (55) (56) can be cast into

$$\left[X_{nm}^{+} \right] = \left[D_{nm} \right] \left[X_m^{-} \right] = \left(\left[\widetilde{D}_{nm} \right] - \frac{1}{2} \left[P_{nm} \right] \right) \left[X_m^{-} \right], \tag{57}$$

here, $\left[\widetilde{D}_{nm} \right]$ corresponds to the Cauchy principal value of the field transmission matrix from block-m to block-n, which can be calculated with numerical integrations. $\left[P_{nm} \right]$ is a Gramm matrix with entries defined by

$$P_{nm}(i,j) = \int_{ti} \vec{\boldsymbol{f}}_{m,j} \bullet \vec{\boldsymbol{f}}_{n,i} \mathrm{d}S \ . \tag{58}$$

Apparently, $\frac{1}{2}\left[P_{nm} \right]$ corresponds to the residual term caused by the singularity of the dyadic Green's function. $P_{nm}(i,j) = 0$ for non-adjacent blocks.

4. Characteristic Basis Functions and Synthetic Basis Functions

Characteristic basis functions (CBFs) (Prakash & Mittra, 2003) are used to further reduce the unknowns in the final linear system. In this example, the CBFs are created in the following way: determine a neighbour domain for each block at first, which consists of N_{adj} nearest blocks. Since the generalized transition matrix of each block is readily available, the scattered fields of the small system consisting of an individual block and its neighbour domain can be calculated easily by solving a small linear equation system as follows,

$$\left[X_m^-\right] - \sum_{n=1, n\neq m}^{N_{adj}} [T_m][D_{mn}]\left[X_n^-\right] = [T_m]\left[X_m^{inc}\right]. \tag{59}$$

The rotated tangential scattered fields (or equivalent surface sources if equation (54) is used.) are then selected as the characteristic basis function of that block, denoted by $\left[X_m^C\right]$, and the total rotated tangential fields are expanded with

$$\left[X^-\right] = \sum_{m}^{N_b} \alpha_m \left[X_m^C\right]. \tag{60}$$

Therefore, equation (53) is cast into a linear system with only N_b unknowns,

$$[A][\alpha] = \left[X_c^{inc}\right]. \tag{61}$$

where the interaction factor between block-m and block-n is defined by

$$A_{mn} = \begin{cases} \left[X_m^C\right]^t \bullet \left([T_m][D_{mn}]\left[X_n^C\right]\right)^*, & \text{for } m \neq n \\ \left[X_m^C\right]^t \bullet \left[X_n^C\right]^*, & \text{for } m = n \end{cases}, \tag{62}$$

and $X_c^{inc}(m) = \left[X_m^C\right]^t \bullet \left[X_m^{inc}\right]^*$. The upper script t stands for transpose operation and * for conjugate.

Synthetic basis functions (Matekovits etal., 2007) can also be applied to reduce the number of unknowns involved in the generalized surface integral equation (53). In order to implement SBFs with GSIE, we have to generate a response space for a block using the method described in (Matekovits etal., 2007), where it is pointed out that the degree of freedom of the SBFs for a block is less than the total unknown number N_m for the block expressed with low-order basis functions. Therefore, based on equivalence principle, an auxiliary source space may be used to handle the effect from all other scatterers in the system except the one under consideration, and it is possible to use SBFs fewer than N_m for that block. This may be considered as an information compression process. The characteristics of the practical structure should be fully made use of in order to achieve a large compression ratio. In radiation problems, the fact that near fields evanesce rapidly from a scatterer is a key factor to use to compress the response space. Hence, the auxiliary

sources should be put as far as possible away from the scatterer under consideration. On the other hand, the input condition and the connecting circuits are all key factors of the problem that may have significant effect on the response space and should be included in the compression procedure. However, the method is hard to implement in cases when sub-blocks are tightly connected, because the auxiliary sources should be put exactly on the interface of a sub-block in these cases. As a result, the compression ratio is usually found to be very low. We have supposed a modified scheme to implement SBFM, which is in somewhat similar to the method described in (Tiberi etal., 2006)). Instead of using point sources, N_s plane waves with incident angles of $\phi_s = 2\pi s/N_s$, $s = 1,\cdots,N_s$ are chosen as the auxiliary sources, as is illustrated in Fig. 10. In cases we have checked, we found that if same number of SBFs are used, this arrangement provides better accuracy than putting auxiliary sources directly on the boundary of the sub-block.

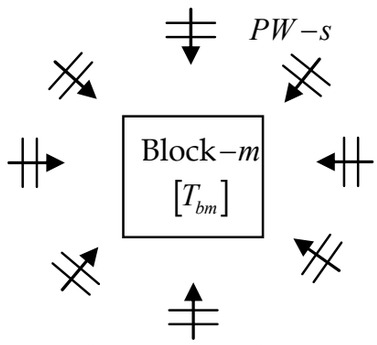

Fig. 10 Auxiliary plane waves are used to generate the SBFs of block-m .

The scattered fields of each incident plane wave are collected together to form a response space of block-m , which is a $N_m \times N_s$ matrix and denoted by $\left[X_{PWm}^{-}\right]$. Applying singular value decomposition (SVD) operation gives

$$\left[X_{PWm}^{-}\right] = [U][S][V]^H . \tag{63}$$

The singular values of $\left[X_{PWm}^{-}\right]$ is stored in the diagonal entries of $[S]$ in descending order, while their corresponding eigen functions are stored in the related columns of $[U]$. We use the following criterion given in (Matekovits etal., 2007) to generate the SBFs,

$$S(p,p)/S(1,1) \le \varepsilon, \quad p = 1,\cdots,N_{svd} . \tag{64}$$

The first N_{svd} eigen functions corresponding to the first N_{svd} singular values are selected as the SBFs of block-m , i.e.,

$$\left[X_{mp}^{sbf}\right] = [U]_p , \qquad p = 1,\cdots,N_{svd} , \tag{65}$$

$[U]_p$ denotes the pth column of $[U]$.

The rotated tangential fields on the reference surface of block-m are then expanded with SBFs as follows,

$$\left[X_m^-\right] = \sum_{p=1}^{N_{svd}} \alpha_{mp} \left[X_{mp}^{sbf}\right]. \tag{66}$$

Substituting (66) into (53) and testing it with SBFs (Galerkin's scheme) result in a size-reduced linear system, the unknown number of which equals to the total number of SBFs on all blocks. The interactions between block-m and block-n are also defined by equation (62), except that SBFs are used to replace CBFs.
In SBFM, because the most significant SBFs for the system are selected once for all, and the mutual coupling is treated rigorously, the numerical accuracy of SBFM is well controlled compared to CBFM.

5. Numerical Results

The field in the cavity illustrated in Fig. 1 is calculated using the above-discussed generalized surface integral equation method. The wall is divided into 36 blocks and the surface of each block is segmented to 40 segments, roughly 10 segments per wavelength. The z-axis polarized TM plane wave with unit magnitude is assumed to excite at Φ= 45°. Triangle-shaped vector basis functions $\vec{f}_{m,i}$ are used to expand all tangential electric field components, while $\hat{a}_n \times \vec{f}_{m,i}$ are used to expand all tangential magnetic field components. The generalized transition matrix of each block is calculated using cascaded network techniques. The total electric fields in the cavity are first calculated using equation (53) directly, with totally 2880 unknowns involved. The calculated electric field is plotted in Fig. 11, from which it can be seen that the fields in the cavity are attenuated from -20dB to -55dB due to the shielding effect of the walls.

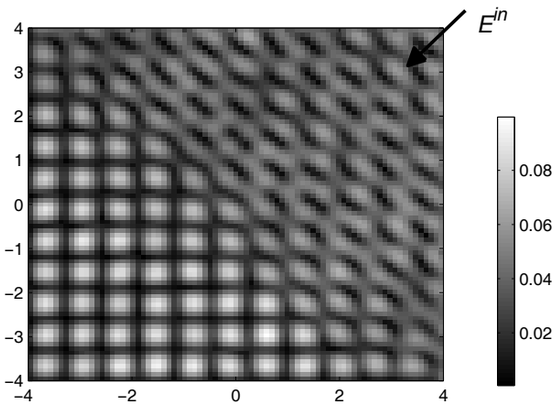

Fig.11. Calculated magnitude (Units: dB) of the total electric field in the internal area of the cavity (8λ×8λ).

Characteristic basis functions are used to re-calculate the field in the cavity. The neighbour domain of each block contains the nearest 3 blocks at one side. Therefore, a small system consisting of 7 blocks has to be solved to create a characteristic basis function. The final

linear system resulting from equation (61) has only 36 unknowns. For large complex multi-scale system, this reduction rate of unknown number is really substantial. For comparison, the discrepancy of the scattered fields in the cavity calculated by using the two methods is plotted in Fig. 12 (in decibels).

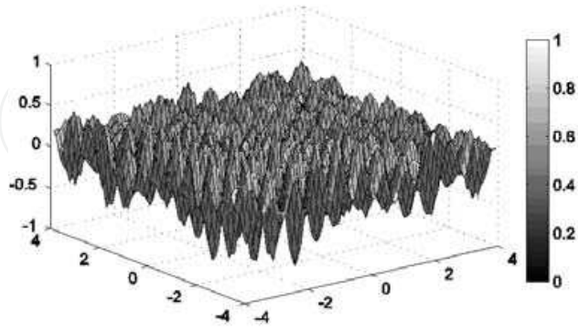

Fig. 12. The discrepancy of the electric fields calculated with the two methods. (Units: dB)

6. Conclusions

A generalized surface integral formulation for analyzing large 2-D cavity with reinforced concrete walls is presented. The wall is divided into small blocks and each block is described by an associated generalized transition matrix defined on its reference surface. Detail structure of each block is analyzed locally only once, and is replaced by a simpler reference surface. By applying the presented method in conjunction with characteristic basis functions and synthetic basis functions, the unknowns and the cost for evaluating the interactions among blocks are significantly reduced.

7. References

Dalke, R. A.; Holloway C. L.; Mckenna P.; Johnsson, M. & Ali, A. S. (2000). Effects of reinforced concrete structures on RF communications. *IEEE Trans. Electromagn. Compat*., Vol. 42, No. 4, (Nov. 2000) 486-496, ISSN 0018-9375.

Creticos, J. P. & Schaubert, D. H. (2006). Electromagnetic scattering by mixed conductor dielectric bodies of arbitrary shape. *IEEE Trans. Antennas Propagat.*, Vol. 54, No. 8, (Aug. 2006) 2402–2407, ISSN 0018-926X.

Lean, M. H. (2004). Novel integral formulation for scattering from multilayered dielectric cylinders of arbitrary cross section. *IEEE Trans. Magnet.* Vol. 40, No. 2, (Mar. 2004) 1476-1479, ISSN 0018-9464.

Li, M. K.; & Chew, W. C. (2007). Wave-field interaction with complex structures using equivalence principle algorithm. *IEEE Trans. Antennas Propagat*., Vol. 55, No. 1, (Jan. 2007) 130-138, ISSN 0018-926X.

Matekovits, L.; Laza, V. A. & Vecchi, G. (2007). Analysis of large complex structures with the synthetic-functions approach. *IEEE Trans. Antennas Propagat.,* Vol. 55, No. 9, (Sept. 2007) 2509-2521, ISSN 0018-926X.

Polewski, M.; Lech, R. & Mazur, J. (2004). Rigorous modal analysis of structures containing inhomogeneous dielectric cylinders. *IEEE Trans. Microw. Theory Tech.*, Vol. 52, No. 5, (May 2004) 1508-1516, ISSN 0018-9480

Prakash, V. V. S. & Mittra, R. (2003). Characteristic basis function method: A new technique for efficent solution of method of moments matrix equations. *Microwave Opt. Technol. Lett.*, Vol. 36, (Jan. 2003) 95–100, ISSN 0895-2477.

Rao, S. M.; Wilton, D. R. & Glisson, A. W. (1982). Electromagnetic scattering by surfaces of arbitrary shape. *IEEE Trans. Antennas Propagat.*, Vol. 30, No. 3, (May 1982) 409–418, ISSN 0018-926X.

Suter. E. & Mosig, J. (2000). A subdomain multilevel approach for the MoM analysis of large planar antennas. *Microwave Opt. Technol. Lett.*, Vol. 26, (Aug. 2000) 270–227, ISSN 0895-2477.

Taskinen, M. & Ylä-Oijala, P. (2006). Current and charge integral equation formulation. *IEEE Trans. Antennas Propagat.*, Vol. 54, No. 1, (Jan. 2006) 58-67, ISSN 0018-926X.

Tiberi, G. A. Manara, M. G. & Mittra, R. (2006). A spectral domain integral equation method utilizing analytically derived characteristic basis functions for the scattering from large faceted objects. *IEEE Trans. Antennas Propagat.*, Vol. 54, No. 9, (Sept. 2006) 2508-2514, ISSN 0018-926X.

Umashankar, K. R.; Taflove, A. & Rao, S. M. (1986). Electromagnetic scattering by arbitrary shaped three-dimensional homogeneous lossy dielectric objects. *IEEE Trans. Antennas Propagat.*, Vol. 34, No.6, (June 1986) 758–766, ISSN 0018-926X.

Waterman, P. C. (2007). The T -matrix revisited. *J. Opt. Soc. Am.* A, Vol. 24, No. 8, (Aug. 2007) 2257-2267, ISSN 1084-7529.

Xiao, G. B.; Mao, J. F. & Yuan, B. (2008). Generalized transition matrix for arbitrarily shaped scatterers or scatterer groups. *IEEE Trans. Antennas Propagat.*, Vol. 56, No.12, (Dec. 2008) 3723–3732, ISSN 0018-926X.

Xiao, G. B.; Mao, J. F. & Yuan, B. (2009). A generalized surface integral equation formulation for analysis of complex electromagnetic systems. *IEEE Trans. Antennas Propagat.*, Vol. 57, No. 3, (Mar. 2009) 701-710, ISSN 0018-926X.

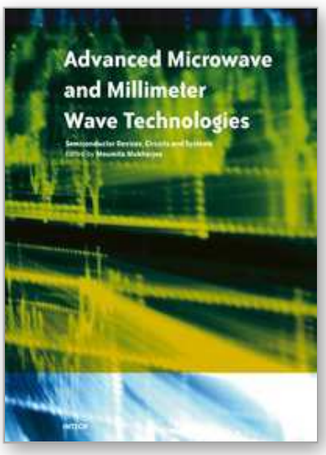

Advanced Microwave and Millimeter Wave Technologies
Semiconductor Devices Circuits and Systems
Edited by Moumita Mukherjee

ISBN 978-953-307-031-5
Hard cover, 642 pages
Publisher InTech
Published online 01, March, 2010
Published in print edition March, 2010

This book is planned to publish with an objective to provide a state-of-the-art reference book in the areas of advanced microwave, MM-Wave and THz devices, antennas and systemtechnologies for microwave communication engineers, Scientists and post-graduate students of electrical and electronics engineering, applied physicists. This reference book is a collection of 30 Chapters characterized in 3 parts: Advanced Microwave and MM-wave devices, integrated microwave and MM-wave circuits and Antennas and advanced microwave computer techniques, focusing on simulation, theories and applications. This book provides a comprehensive overview of the components and devices used in microwave and MM-Wave circuits, including microwave transmission lines, resonators, filters, ferrite devices, solid state devices, transistor oscillators and amplifiers, directional couplers, microstripeline components, microwave detectors, mixers, converters and harmonic generators, and microwave solid-state switches, phase shifters and attenuators. Several applications area also discusses here, like consumer, industrial, biomedical, and chemical applications of microwave technology. It also covers microwave instrumentation and measurement, thermodynamics, and applications in navigation and radio communication.

InTech Europe
University Campus STeP Ri
Slavka Krautzeka 83/A
51000 Rijeka, Croatia
Phone: +385 (51) 770 447
Fax: +385 (51) 686 166

InTech China
Unit 405, Office Block, Hotel Equatorial Shanghai
No.65, Yan An Road (West), Shanghai, 200040, China
中国上海市延安西路65号上海国际贵都大饭店办公楼405单元
Phone: +86-21-62489820
Fax: +86-21-62489821

IntechOpen

IntechOpen